Simulation and Experimental Study of a Synthetic Jet Valveless Pump

Luan Le Van, Tung Thanh Bui, Cuong Nguyen Nhu, An Nguyen Ngoc, Thien Xuan Dinh, Lam Bao Dang, Canh-Dung Tran, Trinh Chu Duc and Van Thanh Dau

Abstract— **A valveless microfluidic pump using a Lead Zirconate Titanate (PZT) diaphragm-actuated synthetic jet is developed and fabricated. For this present design, a valveless pump structure is developed in which the pump chamber is sealed one side and connected to an emitting nozzle at another side. The design is simulated using the multi-physics approach and then successfully investigated with a prototype produced by a low-cost additive fabrication technique. The device's parameters including the pumping liquid characteristics and the size of PZT membrane are optimized based on its desired performance. The developed device can be applied over a wide range of applications from micro-mixing to fluidic controlling.**

Index Terms— **Valveless pump, PZT diaphragm, Synthetic jet**

I. Introduction

DRIVEN by strong developments in several fields such as biomedical science, microelectronics cooling, micro fluid delivery and so on, researches on the microvalve and pump have begun since the 1980s as one of the attractive topics in microelectronics [1]–[3]. Micro-valves are used to control flows in a microchannel by adjusting some device's parameters. Since pumps with movable valve can suffer from several issues, such as dropping of high-pressure across valves, clogged valve when pumping flow of particles, or degradation and fatigue of movable parts [4]–[8]. These drawbacks affect the durability and reliability of devices. Thus, researches on pumps without valves also named as valveless pumps for microsystems have attracted to researchers [9]. The removal of valve from a pump helps eliminate the friction wear, alleviate the sticking effect, yielding a higher reliability of pump. The valveless pump structure also makes a device easily integrated into compact lab-on-a-chip applications [10]–[14]. There are several approaches in which valves were not used in pump structures [15], [16]. One of them is Liebau phenomenon based pumps in which the circulation of a fluid is generated by a periodic compression to handle the direction of the flow in a mechanical system [17]–[19]. This pump structure includes an elastic tubes and a rigid tube connected together in series to form a closed loop. When the elastic tube is periodically squeezed at an asymmetric position of itself, a current through the closed loop is generated. Another popular type of valveless pumps is the peristaltic ones named as the group of reciprocating displacement micro-pumps. For this type, the peristaltic motion of pump chamber is to create a flow in the pump. A driving actuator can be either directly installed insides the pump [20], [21], or designed as an independent mechanism (as a cam or roller) arranged next to the pump chamber [22]. Besides, several other methods to create a flow include generating travelling waves on the pump channel wall [23], applying asymmetric obstacles [24], [25], or combining both previously mentioned methods [26].

The flow rectification in a valveless pump is also another issue that has drawn much attention. The nozzle or diffuser is one of the solutions used to direct the fluid flow instead of a check-valve in micro-pumps. Since the first work on nozzle/diffuser-based pumps [4], various researches on this approach were published [27]–[29]. Recently, a synthetic jet was presented to rectify a fluid flow by a chain of vortexes [30]. For this method, a flow is handled through the interaction of pairs of counter-rotating vortexes at the edge of an orifice generated by an oscillating diaphragm in a sealed cavity [31]–[33]. However, the use of external coil to drive a polydimethylsiloxane (PDMS) membrane with bared magnetic disk is not practically suitable, and resulted in limited pumping performance and practical potentials [30].

In this study, we improved and realized a practical and compact design of a synthetic jet based valveless pump actuated by a commercially available Lead Zirconate Titanate (PZT) diaphragm. For this purpose, the pump chamber is sealed one side and connected to an emitting nozzle at another one. The

Submission date: 2018

Luan Le Van is with the VNU University of Engineering and Technology, Vietnam National University, Hanoi, Vietnam (luanlv@vnu.edu.vn)

Tung Thanh Bui is with the VNU University of Engineering and Technology, Vietnam National University, Hanoi, Vietnam (tungbt@vnu.edu.vn)

Cuong Nguyen Nhu is with the VNU University of Engineering and Technology, Vietnam National University, Hanoi, Vietnam (cuongnn241@vnu.edu.vn)

An Nguyen Ngoc is with the VNU University of Engineering and Technology, Vietnam National University, Hanoi, Vietnam (ngocan@vnu.edu.vn)

Thien Xuan Dinh is with the Graduate School of Science and Engineering, Ritsumeikan University, Shiga 525-8577, Japan (thien@cfd.ritsumei.ac.jp)

Lam bao Dang is with the Hanoi University of Science and Technology, Viet Nam (lam.dangbao@hust.edu.vn)

Canh-Dung Tran is with the School of Mechanical and Electrical Engineering, University of Southern Queensland, Queensland QLD 4350, Australia (Canh-Dung.Tran@usq.edu.au)

Trinh Chu Duc, VNU University of Engineering and Technology, Vietnam National University, Hanoi, Vietnam (trinhcd@vnu.edu.vn)

Van Thanh Dau is with the School of Engineering and Built Environment, Griffith University, Queensland QLD 4222, Australia (v.dau@griffith.edu.au)

designed device is numerically simulated using the multi-physics method and then successfully investigated by experimental work on a prototype fabricated by a low-cost additive manufacturing. Various design parameters including types of liquid and sizes of PZT membrane are considered to optimize the pumping performance, and the efficiency of mixing ability is also demonstrated.

II. Pump Design and Mechanism

A. Pump design

The proposed valveless pump consists of a pump chamber, two inlet and one outlet channels. The inlet and outlet channels are connected with the pump chamber to form a nozzle/diffuser structure at the center of the device as shown in Fig. 1a. The outlet channel is aligned with the central nozzle structure and perpendicular to the two inlets. The cross-section of the outlet is larger than the central nozzle cross-section, but smaller than the inlet channels' one. The whole structure is fabricated by additive technology using relevant plastics.

A conventional pump usually includes only one inlet and one outlet for the distribution of liquid in a system. However, two inlet channels are designed in our synthetic jet valveless pump for not only distributing but also mixing application, which will be discussed in section IIIB.4. The pump chamber is actuated by a PZT membrane, which is an affordable commercial material.

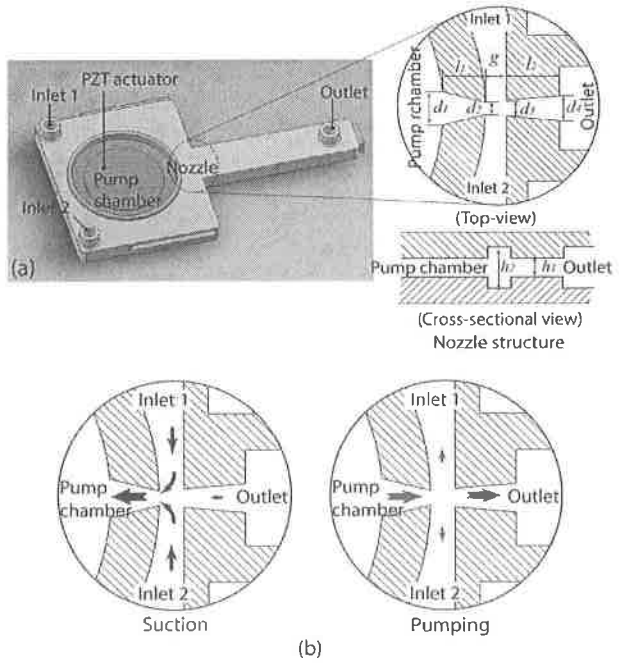

Fig. 1. Design and working principle of the device. (a) Design of the micropump with the zoom-in shows dimensions at the nozzle rectifier. (b) Illustration of the pumping behavior.

During the supply/suction phase, the currents from two inlets, which are closer to the pump nozzle than the outlet, are sucked into the pump chamber. Since the inlet channels are perpendicular to the outlet ones, the coming flow from inlet blocks the backflow by the outlet at the crossing. In addition, the diffuser on the outlet channel also limits the liquid returning from outlet to the pump chamber. The mechanism of suction phase is described in Fig. 1-a. For the pumping phase, the liquid concentrated surrounding the nozzle of pump chamber moves through the nozzle. Based on the Bernoulli's principle, this high-speed outgoing flow drags two fluid inflows into the nozzle and mix them together before moving into outlet channel. Thus, the suction and pumping phases successively occur and push the mixed liquid from inlets to the outlet (Fig. 1b)

B. Governing equations and boundary condition

The pump is modelled by multi-physics simulation in which the transient flow and piezoelectric analyses are carried out using COMSOL Multiphysics©. The fluid flow in pump is considered as incompressible and Newtonian, governed by the Navier-Stokes equation and continuity equation as follows:

$$\rho\left(\frac{\partial u}{\partial t} + u \cdot \nabla u\right) = -\nabla p + \nabla \cdot \mu \nabla u, \quad (1)$$

$$\nabla \cdot u = 0, \quad (2)$$

where u is the velocity, p the pressure, ρ the density, and μ the dynamic viscosity of fluid flow.

With a voltage applied on the piezoelectric diaphragm, the stress and deformation on the diaphragm are expressed by the following stress-strain relations

$$T = c_E S + e^T E, \quad (3)$$

$$D = eS + \epsilon_S E, \quad (4)$$

where T and S are the stress and strain matrices, respectively; E the electric field and D the electric deformation and c_E, e, ϵ_S the elasticity, coupling and permittivity matrices, respectively.

Eq. (3) shows that the stress is partially transferred into electric field while Eq. (4) illustrates the transmission of electric field into the stress as the diaphragm is electrically loaded. The physical properties of materials used in the transient piezoelectric simulation are given in Tab. I.

TABLE I: Physical properties of materials used in transient piezoelectric – FSI simulation

Material	Property	Value
Water	Density (kg/m3)	1000
	Viscosity (mPas)	0.8
Copper	Density (kg/m3	8960
	Young's modulus (Pa)	110×10^9
	Poisson's ratio	0.35
PZT material	Density (kg/m3)	7500
	Matrix of elasticity, coupling and relative permittivity	PZT-5H [39]

The PZT diaphragm clamped at its edge is actuated by an applied voltage $V_{app} = V_o \sin(2\pi f t)$, where V_0 is the amplitude

of the voltage, f the driving frequency. On the surface of PZT diaphragm where a fluid-solid interaction occurs, the fluid velocity is determined as the displacement rate of the movement of the diaphragm with no-slip boundary condition.

The fluidic response inside the pump is simulated using the fluid-structure interaction (*fsi*) and the displacement of the piezo diaphragm by coupling piezoelectric (*solid*) and electrostatics (*es*) modules. Due to the symmetry, a half of the pump is considered as shown in Fig. 2.

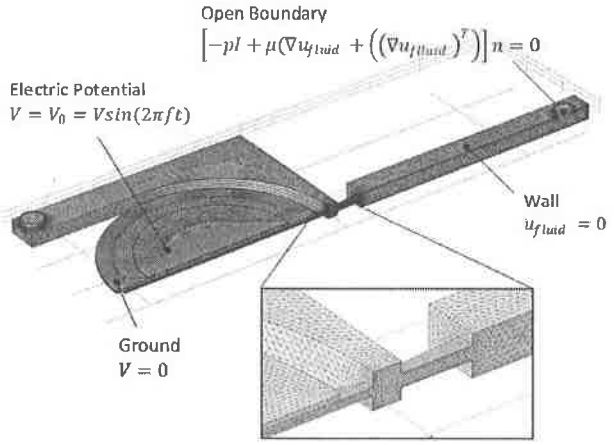

Fig. 2. Meshing and boundary condition setup for the simulation.

A volume of liquid conveyed by the pump from the source to the outlet is determined as the integral of the flowrate at the outlet for an elapsed time as follows.

$$V_{pump} = \iint u_{outlet} \mathrm{d}s\mathrm{d}t \qquad (5)$$

where u_{outlet} is the fluid velocity at the pump outlet and s the cross-section of the outlet.

C. Simulation results

Figure 3a shows the PZT deflection under the applied sinusoidal voltage (V_{app}) with a magnitude (V_o) of 220V. Since the edge of the PZT diaphragm is firmly clamped, the displacement of diaphragm in the X- and Y-directions are neglected, resulting in the domed shape of the deformed PZT diaphragm. The maximum displacement of diaphragm in the Z-direction is around 20 μm. Thus, the pump volume varies with the diaphragm deformation. Numerical results also show that the maximum and minimum volumes of pump are 2.595 mm^3 and 2.575 mm^3 per one operating cycle, respectively. Since the PZT diaphragm is a dielectric and plays the role of a capacitor, a delay of the deflection is observed as the applied voltage changes with time as shown in Fig. 3a.

Figure 3b depicts the velocity of flow at the rectifying nozzle during two working phases where the length and thickness of arrows qualitatively describe the magnitude and direction of flow in the designed channel. As the PZT diaphragm moves upwards, the chamber volume increases, yielding a pressure drop during the suction phase. An inflow created at the nozzle

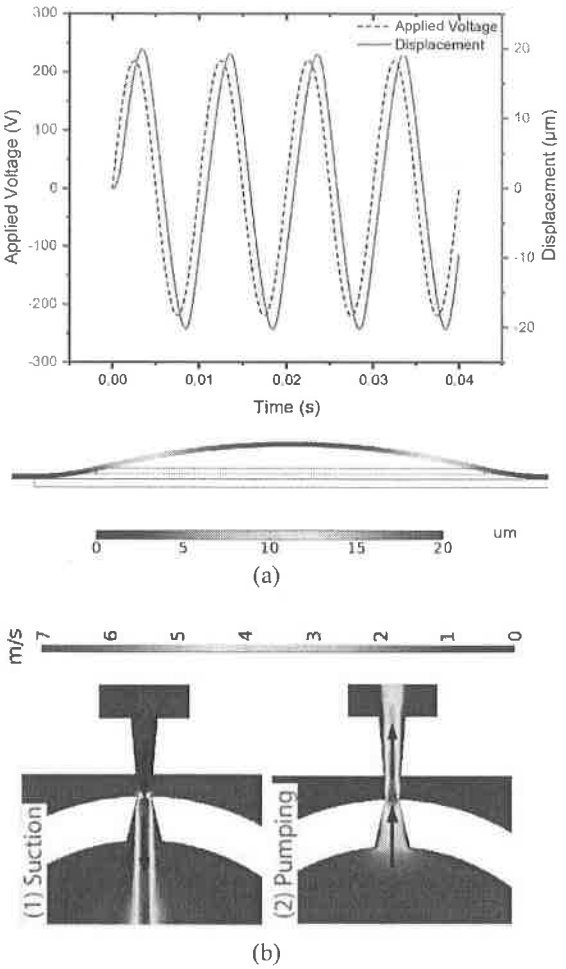

Fig. 3. Simulation results: the fluid-structure (fluid-PZT) interaction illustrates the working principle of micro-pump. (a) Deflection of the diaphragm under sinusoidal applied voltage; (b) The flow velocity at the nozzle of micro-pump at two phases: the highest position (F.3b-(2)) and the lowest position of the membrane (F.3b-(1)) corresponding to the suction and pumping phases, respectively.

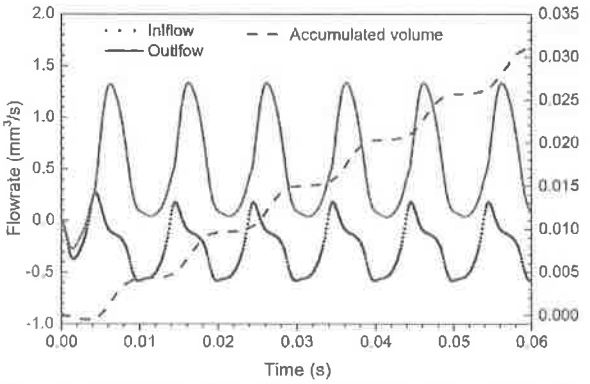

Fig. 4. Simulation result: Time evolution of the pump flow rate at the inlet and outlet with f = 100Hz.

draws fluid into the pump chamber. Inversely, as the chamber pressure increases during the pumping phase, an outflow generated in the chamber propagates into the outlet channel.

The time evolution of pumped volume and flowrates at the inlet and outlet observed by the simulation are shown in Fig. 4. The negative flowrate at the inlet (black line in Fig. 4) indicates an inflow moves into the device. The outflow (red line in Fig. 4) is always positive, inferring that there is almost no backflow even at suction phase as expected from working principle of this design.

TABLE II: Parameters of the valveless pump

Parameter	Value (mm)
PZT diameter D	20
d_1	1.6
d_2	0.6
d_3	0.76
d_4	1.2
l_1	2
l_2	2.5
g	1
h_1	0.5
h_2	1.3

III. EXPERIMENT

A. Experimental setup

The prototype is fabricated using a 3D printing system (Conex3 Objet500, Stratasys). This system uses the polyjet technology with jet layers of liquid photopolymer as thin as 16 microns to produce the prototype with fine details and smooth surfaces [34]. The fabricated pump is shown in Fig. 5 whose parameters are presented in Tab. II.

TABLE III: Physical properties of glycerin - water mixtures at temperature t = 20°c

	A (water)	B (glyceryl:water 1:1 volume:volume)	C (glyceryl:water 2:2 volume:volume)
Viscosity (mPas)	0.8	5.7	14.1
Surface tension (mN/m)	73.2	68.8	67.8
Density (kg/m^3)	1000	1130	1170

Biocompatible glycerin 99.0% (Xilong Scientific Ltd.) is used in our experiments. Due to its solubility and hygroscopic nature, several mixed liquids with different ratios of glycerin and water are used to handle the viscosity and bulk density of liquids. In this work, the liquid of glycerin and water with parameters given in Tab. III is used to evaluate the performance of the present pump prototype.

The experiment setup for the evaluation of pumping performance is illustrated in Fig. 5. The system includes a programmable function generator (Hameg HM 8131-2) which generates sinusoidal signals with a wide range of frequencies on the PZT diaphragm. The generated signal is amplified by an amplifier IC TDA7279 and a transformer with ratio of 1:40. A driving voltage applied on the diaphragm is linearly controlled by the output of the generator.

In order to investigate the pumping effect of the device, two pump inlets are connected to a liquid source while the pump is vertically installed as shown in Fig.6. As soon as a driving voltage is applied, liquid in the outlet rises up, that demonstrates a net driving force is generated in the pumping chamber. Quantitatively, the pump performance is evaluated in terms of the maximum pressure and the pumping flowrate by different driving frequencies.

Experimental results also show that the zero-backpressure flowrate is characterized by adjusting the pumped volume at the outlet while the device is set-up on a horizontal plan. Meanwhile, the backpressure by the variation of the liquid level is observed if both the outlet and inlet are vertically installed as shown in Fig. 5b.

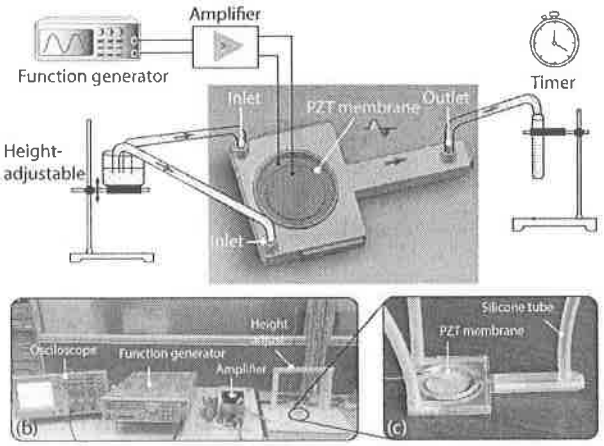

Fig. 5. Experiment setup: (a) Schema of the system including measurement devices; (b) Photo of the experiment setup in laboratory; and (c) Prototype of fabricated valveless microfluidic pump.

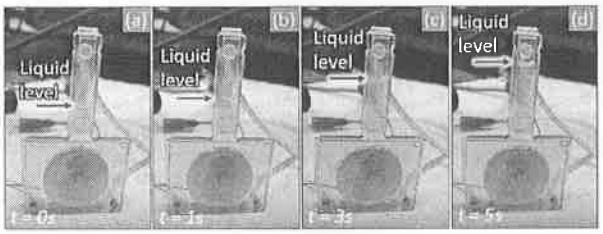

Fig. 6. Investigation of pump operation: raising-up of liquid level in the outlet with time.

B. Results and discussions

1) *Pumping performance*

Three similar pump prototypes were used to investigate and evaluate the performance as well as the repeatability of the designed device. Water is filtered and then introduced into the pump chamber as the working liquid and bubbles of air are completely removed from the chamber to start the experiment. Zero-backpressure flowrate is checked with a range of the driving frequencies from 20 Hz to 400 Hz and the driving

voltage of 220V as shown in Fig. 7.

Starting from a low driving frequency, the flowrate increases with the increase of frequency and reaches a maximum value of about 35 ml/min at the frequency of 100 Hz. The flowrate then reduces to zero-value as the frequency is beyond 400 Hz. Notably, the deviation of flowrate and driving frequency relationship of the three pump prototypes is not significant as found by Fig. 7.

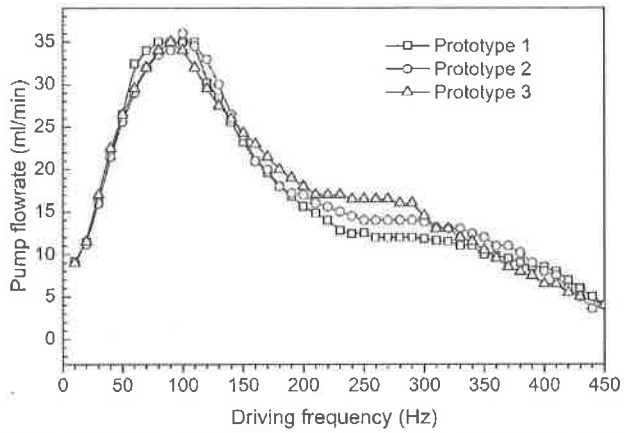

Fig. 7. Relationship of flowrate and driving frequency by experiment using water. Data are collected from three prototypes for repeatability confirmation.

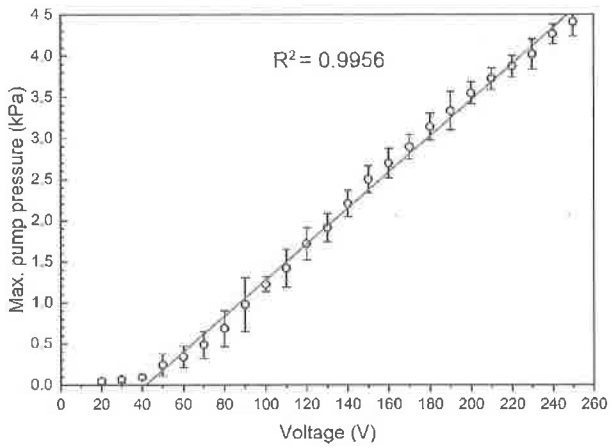

Fig. 8. Maximum pressure plotted versus driving voltage applied on PZT diaphragm (o- line) actuated at the resonant frequency of 100 Hz. Solid line is a linear fit over the range of driving voltages from 40V to 250V.

With the resonant frequency f = 100 Hz corresponding to the maximum flowrate, the backpressure plotted versus driving voltage applied on the diaphragm V_{PZT} by Fig. 8 shows that the stronger driving voltage yields the stronger deflection of diaphragm and then the higher pump pressure. For the present valveless structure, the pumping pressure linearly increases with the driving voltage at a rate of 21 Pa/V and achieved up to 4.5 kPa. It is worth noting that this performance is more preferable than the commercialized counterparts using diaphragms of similar sizes [35], [36].

2) *Pumping with different liquids*

The experiments find that the pumping performance of the present device depends on the viscosity of the medium. In this work, several mixed liquids of different ratios of glycerin and water are used to adjust the liquid viscosity from 0.8mPas to 14.1mPas, while keeping their surface tension and density over an acceptable range as shown in Table 3.

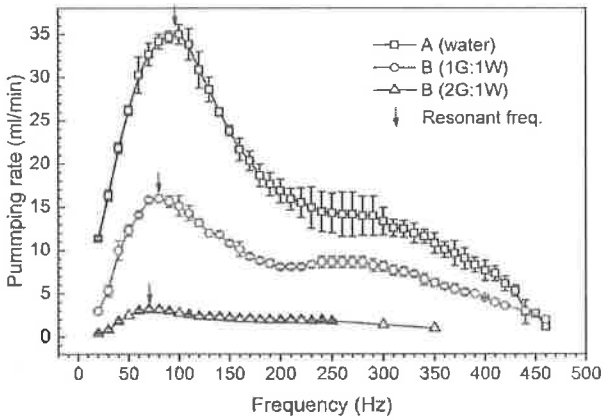

Fig. 9. Pumping rate with different liquids using driving voltage V_o = 220V.

Figure 9 presents the measured pumping rate plotted versus the driving frequency activated by a voltage V_o of 220V using 3 different liquids. Results show that all of the pump characteristics including the driving frequency, resonant frequency and flowrate decrease with the increase of the viscosity and density of the used liquid. In fact, a shift of resonant frequency due to the increasing of the liquid mass inertia results in a lower response to the diaphragm vibration. In other words, the higher viscosity of liquid is, the lower is the frequency required to synchronize with the diaphragm motion.

3) *Effect of the diameter of PZT diaphragm*

The effect of diaphragm size on the pumping performance is also investigated using two commercial diaphragms with the diameters of 20 mm and 35 mm, respectively. For such cases,

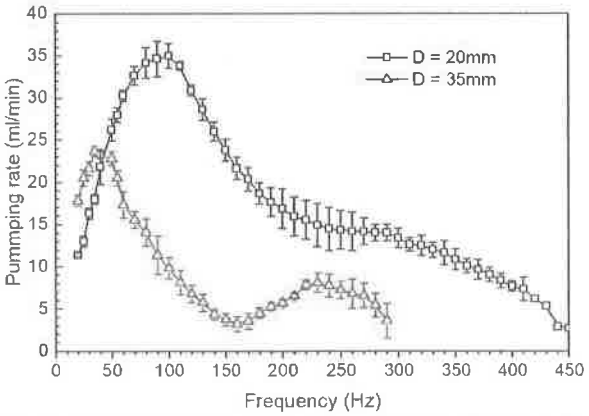

Fig. 10. Experimental results: Impact of PZT diaphragm diameter on the pumping performance: Pumping rate plotted versus the driving frequency with two PZT diaphragm diameters of 20 mm and 35 mm.

dimensions of the pump chamber are modified to fit the diaphragms' sizes whereas the dimensions of inlet channels, nozzle and output channel are unchanged.

The experimental observation by Fig. 10 shows that the resonant frequency tends to shift towards a lower frequency and thus, a smaller value of the maximum pumping rate for larger diaphragm of pump. For example, the consonant frequency and its corresponding maximum rate of pump achieve 40Hz and 24 ml/min; and 100 Hz and 35 ml/min when using diaphragms with diameter of 35 mm and 20 mm, respectively. This result is in good agreement with the finding: "the resonant frequency of diaphragm is reversely proportional to the ratio between the diameter and thickness" stated by Kocbach et al. [37].

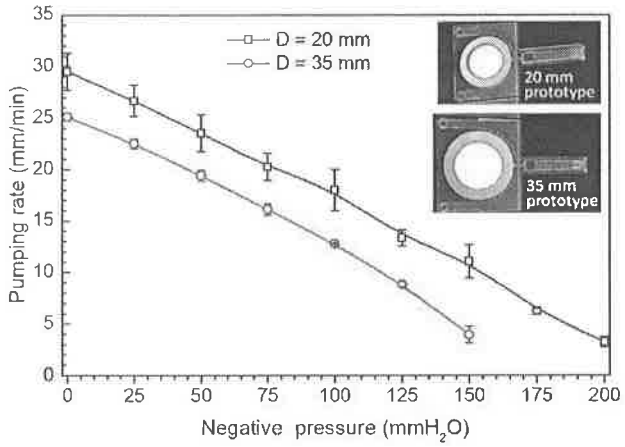

Fig. 11. Experimental results: effect of the PZT diaphragm diameter on the pump's characteristics at resonant frequencies.

Furthermore, by the same applied voltage, a larger diaphragm vibrates with significantly smaller amplitude, thus contribute to decrease the pump flowrate. As a result, the flowrate – back pressure curve of the device using diaphragm of larger diameter moves downward while the gradient of two curves is constant as shown in Fig. 11.

4) *Mixing application*

As mentioned above, the dual-inlet design allows the present pump to be charged of two functions: pumping and mixing of different liquids by two inlets inside the device.

An experiment presented in Fig. 12 a,b&c demonstrated the mixing ability of the device. Dyed waters of blue and red colors are injected into the inlet channels 1 and 2, respectively. The appearance of a third color of water indicates the mixing efficacy of the device. The mixing performance is evaluated by a colour analysis of the mixed liquid created in the outlet channel into hexadecimal triplets (colour codes). The colour codes are then converted into a decimal numerical system. Finally, the decimal numerical results of the mixing liquid flow collected from the nozzle to the downstream of the outlet channel were mapped into a pair of two curves, one for the colour code of the blue liquid (path 1) and another for the red liquid (path 2).

In this work, the mixing efficiency is determined for two cases of voltage, without applied voltage, and 220 V with two different driving frequencies of 10 Hz and 100 Hz. The colour analysis depicts that the mixing efficiency is much better (in terms of occurring faster and stronger) with applied voltage and at higher frequency. Results given in Fig. 12d shows while the dye concentrations of two components are very different from each other without applied voltage (the top and bottom curves), this difference reduces with the applied voltage of 220 V. Specially, the mixing liquid achieves the homogeneity in colour at the higher driving frequency of 100 Hz (curves 5 & 6 – Fig. 12d). This is demonstrated by Fig. 9 in which the pump's efficiency achieves optimum at the frequency of f = 100Hz.

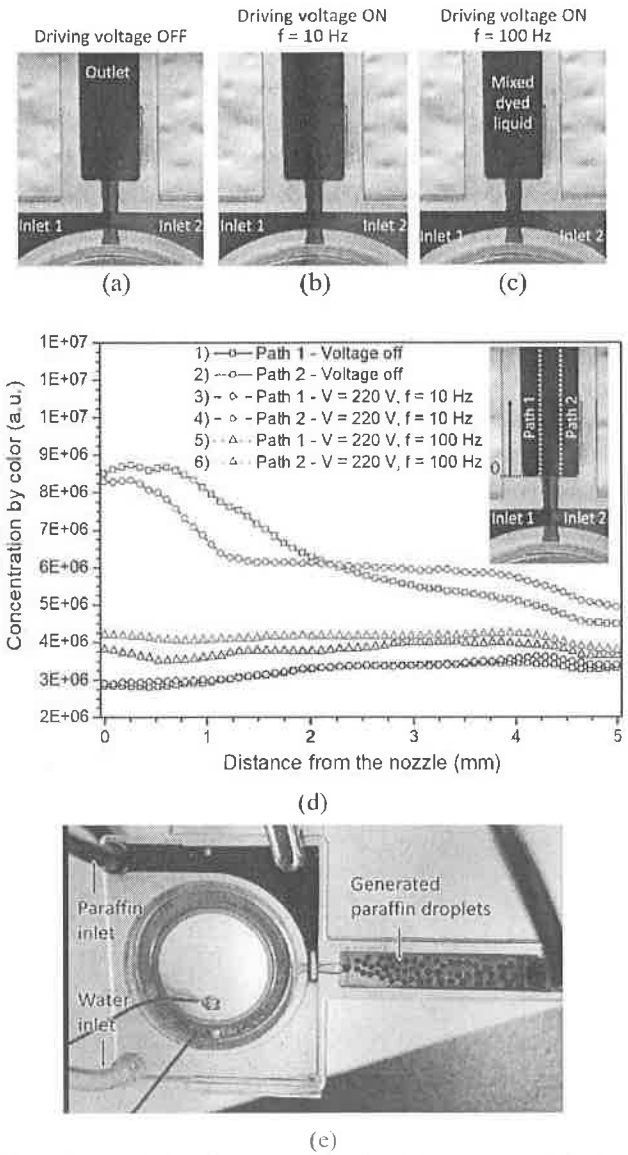

Figure 12. Application of the present pump in mixing two coloured liquids (a), (b) & (c): Colour of mixed liquid in the outlet channel without the applied voltage, and with the applied voltages of 220V-10Hz and 220V-100Hz, respectively, (d) Evolution of concentration of liquid components by colour code in the outlet channel with respect to the distance from the nozzle. (e) Experiment of mixing two immiscible liquids (water and dyed paraffin): the immiscible liquids are mixed into micro droplet.

Notably, the mixing was also observed between two immiscible liquids. For example, dyed paraffin liquid and water are introduced into the device through two inlet channels as shown in Fig. 12e. These liquid components are pumped and mixed into a suspension of paraffin. After going through the emitting nozzle paraffin is divided into micro-droplets of different sizes. For such mixing experiment, results by Li and Barrow [38] showed that the droplet size depends on the properties, the surface tension and viscosity of two liquids, and the applied voltage and driving frequency. For the present approach, the nozzle geometry can be adjusted to control the droplet size as well as the generating rate of the system. For example, an asymmetric inlet nozzle or multi-inlets can be introduced to generate complex droplets. This technique is implemented to lab-on-chips or multifunctional fluidic platforms and the problem will be addressed in our next work.

IV. Conclusions

In this paper, a miniaturized valveless pump actuated by a PZT diaphragm coupled with the synthetic jet principle to handle fluid flows is developed. A prototype of the proposed pumping device was fabricated using a 3D printer. The characterization and performance of the present pump was investigated by both the simulation and experiment. Effects of the engineering parameters of pump including dimensions and working liquid on its performance was also evaluated. Results shown a linear increase of the pump performance with the applied voltage as well as the impact of used liquid on the pump characteristics. Experimental results also revealed that the present device can work with a broad range of driving frequency and voltage magnitude. Finally, with the mixing ability applicable for both miscible and immiscible liquids, the developed pump is promised as a potential micro-droplet generator in various applications.

References

[1] Y.-N. Wang and L.-M. Fu, "Micropumps and biomedical applications – A review," *Microelectron. Eng.*, vol. 195, pp. 121–138, Aug. 2018.

[2] F. Abhari, H. Jaafar, and N. A. Md Yunus, *A comprehensive study of micropumps technologies*, vol. 7, no. 10, 2012.

[3] D. J. Laser and J. G. Santiago, "A review of micropumps," *J. Micromechanics Microengineering*, vol. 14, no. 6, pp. R35–R64, 2004.

[4] E. Stemme and G. Stemme, "A valveless diffuser/nozzle-based fluid pump," *Sensors Actuators A. Phys.*, vol. 39, no. 2, pp. 159–167, 1993.

[5] B. Fan, G. Song, and F. Hussain, "Simulation of a piezoelectrically actuated valveless micropump," *Smart Mater. Struct.*, vol. 14, no. 2, pp. 400–405, 2005.

[6] P. Woias, "Micropumps—past, progress and future prospects," *Sensors Actuators B Chem.*, vol. 105, no. 1, pp. 28–38, 2005.

[7] C. Noergaard, E. L. Madsen, J. M. T. Joergensen, J. H. Christensen, and M. M. Bech, "Test of a Novel Moving Magnet Actuated Seat Valve for Digital Displacement Fluid Power Machines," *IEEE/ASME Trans. Mechatronics*, vol. 23, no. 5, pp. 2229–2239, 2018.

[8] D. B. Roemer, M. M. Bech, P. Johansen, and H. C. Pedersen, "Optimum Design of a Moving Coil Actuator for Fast-Switching Valves in Digital Hydraulic Pumps and Motors," *IEEE/ASME Trans. Mechatronics*, vol. 20, no. 6, pp. 2761–2770, 2015.

[9] V. T. Dau, T. X. Dinh, Q. D. Nguyen, R. Amarasinghe, K. Tanaka, and S. Sugiyama, "Microfluidic valveless pump actuated by electromagnetic force," *Proc. IEEE Sensors*, no. Type II, pp. 679–682, 2009.

[10] H. K. Ma, R. H. Chen, N. S. Yu, and Y. H. Hsu, "A miniature circular pump with a piezoelectric bimorph and a disposable chamber for biomedical applications," *Sensors Actuators, A Phys.*, vol. 251, pp. 108–118, 2016.

[11] D. J. Thomas, Z. Tehrani, and B. Redfearn, "3-D printed composite microfluidic pump for wearable biomedical applications," *Addit. Manuf.*, vol. 9, pp. 30–38, 2016.

[12] P. Kawun, S. Leahy, and Y. Lai, "A thin PDMS nozzle/diffuser micropump for biomedical applications," *Sensors Actuators, A Phys.*, vol. 249, pp. 149–154, 2016.

[13] B. Zhao, X. Cui, W. Ren, F. Xu, M. Liu, and Z. G. Ye, "A Controllable and Integrated Pump-enabled Microfluidic Chip and Its Application in Droplets Generating," *Sci. Rep.*, vol. 7, no. 1, pp. 1–8, 2017.

[14] J. Wang, A. J. Mcdaid, C. Lu, and K. C. Aw, "A Compact Ionic Polymer-Metal Composite (IPMC) Actuated Valveless Pump for Drug Delivery," *IEEE/ASME Trans. Mechatronics*, vol. 22, no. 1, pp. 196–205, 2017.

[15] B. D. Iverson and S. V. Garimella, "Recent advances in microscale pumping technologies: A review and evaluation," *Microfluid. Nanofluidics*, vol. 5, no. 2, pp. 145–174, 2008.

[16] T. Zhang and Q. M. Wang, "Performance evaluation of a valveless micropump driven by a ring-type piezoelectric actuator," *IEEE Trans. Ultrason. Ferroelectr. Freq. Control*, vol. 53, no. 2, pp. 463–473, 2006.

[17] G. Liebau, "Über ein ventilloses Pumpprinzip," *Naturwiss.*, vol. 41, p. 327, 1954.

[18] T. T. Bringley, S. Chilress, N. Vandenberghe, and J. Zhang, "An experimental investigation and a simple model of a valveless pump," *Phys. Fluids*, vol. 20, no. 3, pp. 1–15, 2008.

[19] A. I. Hickerson and M. Gharib, "On the resonance of a pliant tube as a mechanism for valveless pumping," *J. Fluid Mech.*, vol. 555, pp. 141–148, 2006.

[20] B. Pečar, D. Križaj, D. Vrtačnik, D. Resnik, T. Dolžan, and M. Možek, "Piezoelectric peristaltic micropump with a single actuator," *J. Micromechanics Microengineering*, vol. 24, no. 10, 2014.

[21] L. S. Jang, K. Shu, Y. C. Yu, Y. J. Li, and C. H. Chen, "Effect of actuation sequence on flow rates of peristaltic micropumps with PZT actuators," *Biomed. Microdevices*, vol. 11, no. 1, pp. 173–181, 2009.

[22] K. B. Vinayakumar, G. Nadiger, V. R. Shetty, N. S. Dinesh, M. M. Nayak, and K. Rajanna, "Packaged peristaltic micropump for controlled drug delivery application," *Rev. Sci. Instrum.*, vol. 88, no. 1, 2017.

[23] J. Ogawa, I. Kanno, H. Kotera, K. Wasa, and T. Suzuki, "Development of liquid pumping devices using vibrating microchannel walls," *Sensors Actuators, A Phys.*, vol. 152, no. 2, pp. 211–218, 2009.

[24] H. J. Sheen *et al.*, "Unsteady flow behaviors in an obstacle-type valveless micropump by micro-PIV," *Microfluid. Nanofluidics*, vol. 4, no. 4, pp. 331–342, 2008.

[25] C. J. Lee, H. J. Sheen, Z. K. Tu, U. Lei, and C. Y. Yang, "A study of PZT valveless micropump with asymmetric obstacles," *Microsyst. Technol.*, vol. 15, no. 7, pp. 993–1000, 2009.

[26] H. Afrasiab, M. R. Movahhedy, and A. Assempour, "Proposal of a new design for valveless micropumps," *Sci. Iran.*, vol. 18, no. 6, pp. 1261–1266, 2011.

[27] T. X. Dinh, N. T. M. Le, V. T. Dau, and Y. Ogami, "A dynamic model for studying valveless electromagnetic micropumps," *J. Micromechanics Microengineering*, vol. 21, no. 2, p. 025015, Feb. 2011.

[28] A. Chandrasekaran and M. Packirisamy, "Geometrical tuning of microdiffuser/nozzle for valveless micropumps," *J. Micromechanics Microengineering*, vol. 21, no. 4, 2011.

[29] S. F. Hwang and Y. M. Ji, "Experimental investigation on the design of nozzle/diffuser for micropumps," *Int. J. Precis. Eng. Manuf.*, vol. 15, no. 4, pp. 717–723, 2014.

[30] N. Q. Dich, T. X. Dinh, P. H. Pham, and V. T. Dau, "Study of valveless electromagnetic micropump by volume-of-fluid and OpenFOAM," *Jpn. J. Appl. Phys.*, vol. 057201, no. 5, p. 057201, May 2015.

[31] B. L. Smith and G. W. Swift, "A comparison between synthetic jets and continuous jets," *Exp. Fluids*, vol. 34, no. 4, pp. 467–472, 2003.

[32] N. K. Yamaleev and M. H. Carpenter, "A Reduced-Order Model for Efficient Simulation of Synthetic Jet Actuators," *NASA Rep. NASA/TM*, no. December, p. 212664, 2003.

[33] V. T. Dau, T. X. Dinh, and S. Sugiyama, "A MEMS-based silicon micropump with intersecting channels and integrated hotwires," *J. Micromechanics Microengineering*, vol. 19, no. 12, p. 125016, Dec. 2009.

[34] "PolyJet | 3D Printing Solutions | Stratasys Direct Manufacturing." [Online]. Available: https://www.stratasysdirect.com/solutions/polyjet/. [Accessed: 18-Oct-2017].

[35] Takasago fluidics micropump, "Piezoelectric Micro Pump - Takasago Fluidic Systems."

[36] Curie Jet Micropump, "CurieJet® Liquid/Gas Micro Pump :: Micro Fluidics Pump, Micropump."

[37] J. Kocbach, P. Lunde, and M. Vestrheim, "Tables of resonance frequencies for disks of PZT-5A, PZT-5H, Pb(ZrTi)O3 and PbTiO3," 2000.
[38] J. Li and D. A. Barrow, "A new droplet-forming fluidic junction for the generation of highly compartmentalised capsules," *Lab Chip*, vol. 17, no. 16, pp. 2873–2881, 2017.
[39] "Piezoacoustic Transducer," [Online]. Available: https://www.comsol.com/model/piezoacoustic-transducer-1477. [Accessed: 23-Oct-2018].

Luan Le Van receiver the B.S. and M.E degreees in Electronics from Hanoi University of Science and Technology in 1999 and 2003, respectivelly. Currently, he is working toward his PhD degree at the VNU University of Engineering and Technology, Vietnam. His research interests include electronic biosensor, valveless micro pump and microfludic.

Tung Thanh Bui received the B.S. degree in electrical engineering from Vietnam National University, Hanoi (VNUH) in 2004, and the M.E. and D.Eng. degrees in Science and Engineering from Ritsumeikan University, Shiga, Japan, in 2008 and 2011, respectively.
From 2011 to 2015 he was a Post-doctoral Researcher with the 3D Integration System Group, Nanoelectronics Research Institute (NeRI), National Institute of Advanced Industrial Science and Technology (AIST), Tsukuba, Japan.
Currently, he is an assistant professor at the Faculty of Electronics and Telecommunication (FET), University of Engineering and Technology (UET), Vietnam National University, Hanoi (VNUH). His current interests include MEMS based sensors, actuators and applications.

Cuong Nguyen Nhu received the BS in Electronics and Telecommunications from University of Engineering and Technology (UET), Vietnam National University, Hanoi (VNU-H) in 2018. He is currently researching at Laboratory of Micro-Electro-Mechanical Systems and Micro Systems – University of Engineering and Technology, VNU. His main research interests include microfluidics, MEMS based sensors, actuators and applications.

An N. Nguyen (S'11) received the B.E. in telecommunication engineering from Hanoi University of Science and Technology in 2011. He received the M.E. and the Ph.D. degrees in electrical, electronic and communication engineering from Chuo University, Japan, in 2014 and 2017, respectively. Since April 2017, he has been with University of Engineering and Technology-VNU, Hanoi, Vietnam, where he is currently a lecturer. His current research interests include micropump, sensors and material characterization using free space techniques.

Thien Xuan Dinh received the B.S. degree in aerospace engineering from Hochiminh City University of Technology in 2002, Vietnam and the M.Sc. and Ph.D. degrees in mechanical engineering from Ritsumeikan University in 2004 and 2007, respectively. He was recipient of Japan Government Scholarship (MEXT) for Outstanding Student to pursuits his M. Sc. and Ph. D. courses and Japan Society for the Promotion of Science postdoctoral fellowship from 2011 to 2013.
His general research interest is computation of fluid flow. The large parts of his research are turbulence modeling using Large Eddy Simulation, multiphase modeling using Volume of Fluid technique, and simulation of turbulence and dispersion. Recently, he has focused on computation of fluid flow for developing microfluidic devices as microsensors, micropump, and micromixer for biochemical engineering.

Dang Bao Lam received the Eng. degree from Slovak University of Technology (1998), the M.E. degree in Mechanics of Machines (2004), and the D.Eng. degree in MEMS engineering from Hanoi University of Science and Technology (2015). He has been a lecturer in a School of Mechanical Engineering, HUST since 2001. His current interests include MEMS based sensors, actuators and applications.

Canh-Dung Tran (CD Tran) is Associate Professor at School of Mechanical and Electrical Engineering, Faculty of Health, Engineering and Sciences, Senior Research Fellow of the Computational Engineering Scientific Research Centre, The University of Southern Queensland (USQ), Australia. He was a Visiting Research Fellow at the Department of Mechanical Engineering, National University of Singapore (NUS, 2017) and the Nanotech Institute, University of Texas, Dallas (UTD, 2014).
From 2005 to 2010, he was a Research Scientist and Project Leader at the CSIRO (Australia) and participated in various projects relating to modelling and analyzing the mechanical behavior of materials. He has gained wide experience in developing mechanical, material engineering and Carbon Nano-tube research proposals, which were funded internally and externally, in conjunction with the CSIRO, UTD, NUS, University of Sydney (Australia) and the University College of London (UK).
He has produced 120 research publications as author and co-authors in the areas of numerical simulation including stochastic macro-micro methods, advanced Fibrous Materials, nanomaterials, CNTs and NEMS.

Trinh Chu Duc received the B.S. degree in physics from Hanoi University of Science, Hanoi, Vietnam, in 1998, the M.Sc. degree in electrical engineering from Vietnam National University, Hanoi, in 2002, and the Ph.D. degree from Delft University of Technology, Delft, The Netherlands, in 2007. His doctoral research concerned piezoresistive sensors, polymeric actuators, sensing microgrippers for microparticle handling, and microsystems technology. He is currently an Associate Professor with the Faculty of Electronics and Telecommunications, University of Engineering and Technology, Vietnam National University, Hanoi, Vietnam. He has been chair of Microelectromechanical Systems and Microsystems Department, since 2011.

Van Thanh Dau received the B.S. degree in aerospace engineering from Hochiminh City University of Technology, Vietnam, in 2002, and the M.S. and Ph.D. degrees in micro-mechatronics from Ritsumeikan University, Japan, in 2004 and 2007, respectively.
From 2007 to 2009, he was a Postdoctoral Fellow with Japan Society for the Promotion of Science (JSPS) at Micro Nano Integrated Devices Laboratory, Ritsumeikan University. From

2010-2018 he was a research scientist at Sumitomo Chemical Co., Japan, where he worked on integrated micro electrospray and atomization methods. Currently, he is a Lecturer at School of Engineering and Built Environment, Griffith University, Australia.

His research subjects are microfluidics, electrofluidodynamics and micromechatronics. He is the author and co-author of more than 100 scientific articles and 25 inventions.